GeoVirtual 2020 September 14-16
Resilience and Innovation

Water balance in filtered tailings storage facilities: laboratory tests and numerical simulations

AYANG NZAME, L [1,2]., PABST, T. [1,2] & MARTIN, V.[3]
[1]*Department of Civil, Geological, and Mining Engineering, Polytechnique Montréal, P.O. Box 6079, Succ. Centre-ville, Montréal, QC H3C 3A7, Canada*
[2] *RIME- Research Institute of Mines and Environment.*
[3]*Golder Associates Ltd., Montréal, Quebec, Canada*

ABSTRACT
Filtered tailings are often considered a promising alternative to conventional deposition methods and may contribute to improve the geotechnical stability of tailings storage facilities. However, the risk of generation of acid mine drainage (AMD) or contaminated neutral drainage (CND) can be increased by desaturation if the tailings are reactive. The objective of this study was to evaluate the influence of layer thickness and compaction on the hydrogeological behaviour of filtered tailings. Laboratory column tests were conducted. Volumetric water content (θ), suction (ψ), air temperature, relative humidity and evaporation rates were monitored during wetting and drying cycles. The preliminary results obtained in this study showed that there was no significant influence of thickness of the deposition layers on the behaviour of tailings. The development of a layer of salts at the surface of the tailings influences the evaporation rate and contributed to maintain a higher degree of saturation than expected.

RÉSUMÉ
Les résidus filtrés sont souvent considérés comme une alternative prometteuse aux méthodes de déposition conventionnelles et peuvent contribuer à améliorer la stabilité géotechnique des aires d'entreposage des résidus. Cependant, le risque de génération de drainage minier acide (DMA) ou de drainage neutre contaminé (CND) peut être accru par la désaturation si les résidus sont réactifs. L'objectif de cette étude était d'évaluer l'influence de l'épaisseur et de la compaction des couches de résidus filtrés sur leur comportement hydrogéologique. Des essais en colonne ont été réalisés au laboratoire. La teneur en eau volumique, la succion, la température, l'humidité relative et les taux d'évaporation ont été mesurés pendant les cycles de mouillage-séchage. Les résultats préliminaires obtenus dans cette étude montrent qu'il n'y avait pas d'influence significative de l'épaisseur sur le comportement des résidus. Le développement d'une couche de sels à la surface influençait le taux d'évaporation et permettait de maintenir un degré de saturation plus élevé qu'attendu.

1 INTRODUCTION

Mining operations generate large volumes of liquid and solid wastes. Tailings, produced from the concentration of ore, represent a significant fraction of the wastes produced. They are typically stored on the surface in tailings storage facilities (Spitz et Trudinger, 2009). Pulp tailings are usually transported hydraulically by pipeline. High pore pressures can develop in the storage facilities, thus reducing shear resistance and eventually leading to dams failures (James et al., 2013). Although there are many reasons for these ruptures, including slope and foundation instability, internal erosion, surface erosion, peak exceedances and seismic damage (Azam et Li, 2010)., water is usually a key factor (Strachan et Goodwin, 2015).

The reduction of tailings water content can limit the risk of instability (Robinsky, 1975; Fourie 2012b). Tailings produced in the form of pulp can be densified with additives, thickeners, cyclones, filters or pumps. The pulp density (P) can then reach 60% or more, allowing densified tailings to be classified into three categories: thickened tailings, paste tailings and filtered tailings. (Martin et al., 2018).

Filtered tailings are increasingly considered by mining companies. They are allowing also minimize the needs for dams and settling pond (Robinsky, 1999). However, tailings often contain leachable metals and/or are potentially acid generating, and therefore require specific management to prevent contaminated mining drainage generation.

Acid mine drainage (AMD) occurs when sulfurous minerals (mainly pyrite and pyrrhotite) contained in the tailings come into contact with water and air (Lindsay et al., 2015). Oxidation of reactive sulfides leads to the generation of sulfuric acid, which lowers the pH and increases the solubility of metals (Bouzahzah, 2013). AMD is characterized by low pH and high concentrations of metals and sulfates (Aubertin et al. 2002a; Nordstrom et al. 2015).

AMD generation control methods for reclamation of the tailing pond commonly include the construction of

various types of covers such as capillary barrier effect covers (CCBE; Aubertin et al., 1996); single-layer covers (Maqsoud et al., 2013; Pabst, 2017) or water covers. The objective of these cover systems is usually to control oxygen migration by maintaining a high degree of saturation in tailings or cover materials (Bussière., 2007). Oxygen diffusion in water or saturated granular materials is indeed 10 000 slower than in air (Aachib et al., 2004).

In the absence of cover during the operation phase, reactive filtered tailings can oxidize, making site reclamation more complex (Pabst et al., 2018). Water balance in situ therefore needs to be controlled to limit AMD generation while maintaining high mechanical properties. Several approaches were proposed to optimize water balance. For example, a reduction of porosity (i.e. an increase of dry density) can contribute to increase water retention capacity. A well-planned deposition design could also prevent desaturation of tailings by evaporation by continuously adding newly produced tailings on top of the storage facility (Martin, 2018).

This article describes some of the preliminary laboratory work conducted to evaluate the impact of the thickness and compaction of the layers during deposition on the hydrogeological behavior of the filtered tailings

2 MATERIALS AND METHOD

2.1 Tailings geotechnical and hydrogeological properties

Mine tailings were sampled at a partner mining operation located in Abitibi-Témiscamingue in western Quebec. Tailings were homogenized and characterized in the laboratory. The tailings relative particle density was measured according to ASTM D854-14 (2014) and D_r = 2.92. The particle size distribution was evaluated in according to ASTM D7928-17 (2017b). Test was carried out with 5 duplicates. The Fredlund model (2000) was used to adjust the curve. Measured D10 and D60 for the tailings were respectively 0.003 mm and 0.035 mm corresponding to 10% and 60% of particles passing on the cumulative curve (Figure 1). The water retention curve of the tailings was measured using a pressure plate extractor (ASTM D6836 2016). The van Genuchten model was used to adjust the curve (Figure 2). Tailings saturated hydraulic conductivity (k_{sat}) was measured using flexible wall permeameters (ASTM D5084-16, 2016b). Two tests were carried out and the geometric average value of the saturated hydraulic conductivity was $k_{sat} = 3\times10^{-7}$ m/s.

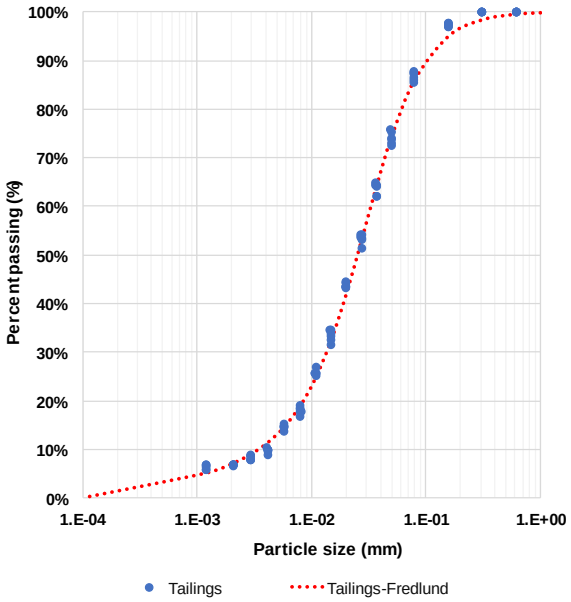

Figure 1. Grain size distributions of the tailings

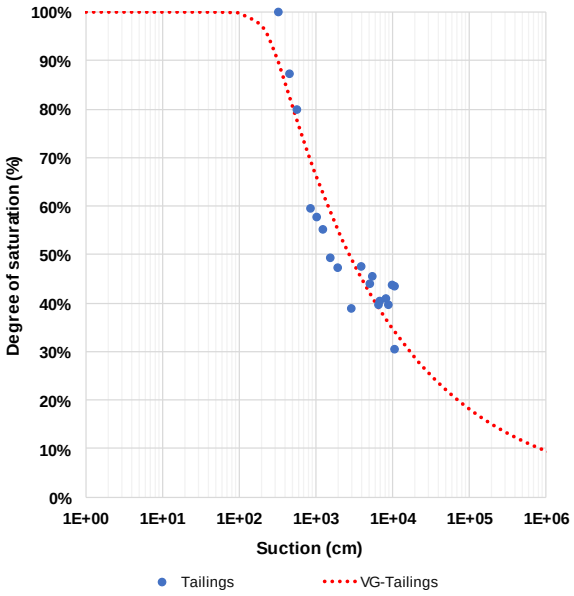

Figure 2. Water retention curve of tailings

2.2 Chemical and mineralogical properties

The bulk chemical composition of the tailings was determined by inductively coupled plasma atomic emission spectrometry (ICP-AES). Total sulfur (S) and carbon (C) were also measured with an induction furnace. The acid-base accounting (ABA) parameters were calculated using total sulfur and carbon contents (Morin and Hutt., 2001; MEND., 2009). A total of five samples were characterized. The presented results (Table 1) are the averages obtained for each parameter. Tailings contained relatively high concentrations of sulfur (9.07%) and low concentrations of carbon (0.3%), resulting in an elevated acid-generation potential ($AP = \%S_{total} \times 31.25$) and a low neutralization potential ($NP = \%C_{inor} \times 83.3$).

Mineralogical phases were identified by X-ray diffraction (XRD). Results for sulfide and carbonate minerals were reconciled with chemical analyses (Table 1). Pyrite and dolomite represented 14.4% and 2.19%, respectively. Additionally, 2.14% gypsum 0.13% arsenopyrite and traces of sphalerite were detected in the tailings.

Table 1. Sulfur/carbon concentrations, acid-base accounting parameters, and XRD main results.

Parameter	Averages
S_{total} (%)	9.07
AP (KgCaCO3 eq/t)	283.5
C_{total} (%)	0.29
NP (KgCaCO3 eq/t)	24.2
NNP (NP-AP) (KgCaCO3 eq/t)	-259.3
NPR (NP/AP)	0.10
Pyrite (%)	14.4
Dolomite (%)	2.19
Gypsum (%)	2.24
Other minerals, in order of importance: quartz, muscovite, anorthite, chlorite, muscovite, sanidine, albite, (%)	81

3 COLUMN TESTS

3.1 Column setup

The aim of the column tests was to assess the impact of the thickness and compaction of the deposition layers on the hydrogeological behavior of the filtered tailings. Laboratory experiments were carried out in four columns with an internal diameter of 36 cm and a height of up to 70 cm.

The tailings in-situ dry density was approximately 1670 kg/m^3, corresponding to the expected density in situ. Tailings were compacted in successive layers (7.5 cm thick) at an average porosity of 0.43. The desired final thicknesses were 15 cm; 30 cm; 45 cm and 60 cm in columns C15, C30, C45 and C60 respectively (Table 2)

Table 2. Characteristics of the column tests conducted in the laboratory where $H_{columns}$: column height; $D_{columns}$: column diameter; $H_{tailings}$: tailings height; n: porosity; e: void ratio; θ: initial volumetric water content ; S_r: initial degree of saturation

Parameter	C15	C30	C45	C60
$H_{columns}$ (cm)	70	70	70	85
$D_{columns}$ (cm)	36	36	36	36
$H_{Tailings}$ (cm)	15.6	31.5	46	62
n (-)	0.432	0.437	0.422	0.428
e (-)	0.76	0.78	0.73	0.75
θ (-)	0.298	0.295	0.303	0.3
Sr (%)	69	68	72	70

A perforated plate was placed 10 cm from the bottom of each column. The plate was covered with a geotextile. The 10 cm gap allowed the drainage waters to be collected. Outlet was connected to a 4-litre container to sample drainage water. Volumes and water quality were measured regularly.

The columns were instrumented with volumetric water content sensors (EC-5) and suction probes (Watermark-Irrometer) placed every 15 cm. Each column was placed on a scale to monitor the evolution of the mass and to evaluate the water balance during the test. (Figure 3).

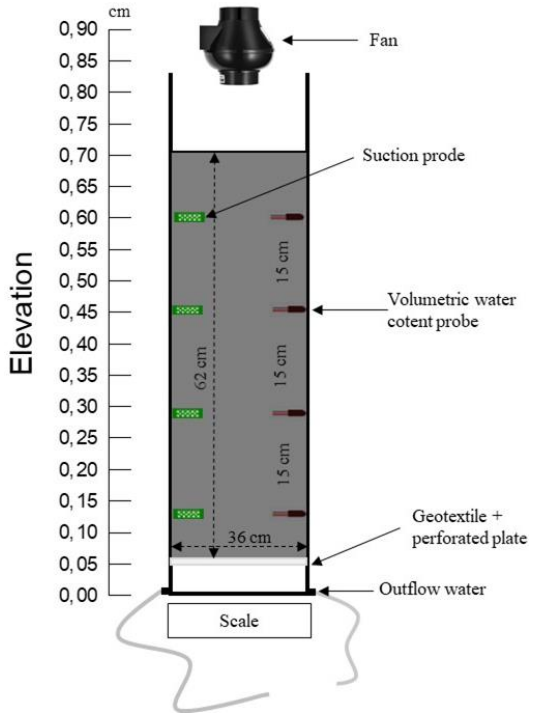

Figure 3. Column configuration (here C60) and instrumentation

3.2 Instrumentation

A specific probe calibration was performed for each sensor (Figure 4). The calibration curve (Eq.1) was applied to the EC-5 probes measurements:

$$\theta_{calibrated} = 0.77 * \theta_{measured} + 0.003 \quad \text{(Eq.1)}$$

The calibrated volumetric water content values were subsequently adjusted to account for tailings maximum porosity in each column.

The pore water pressure was measured with Watermark probes (Irrometer Company, Inc.) placed in the tailings at the same locations as the water content sensors. These sensors can measure suction between 1 and 200 kPa with an accuracy of 1 kPa.

The pore water pressure and water content were recorded every 30 minutes. Mass of each scale were recorded every 10 minutes to evaluate the water balance during the test.

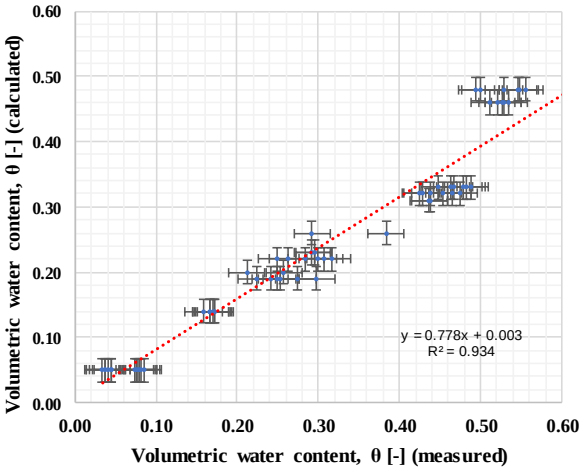

Figure 4. Calibration curve of EC-5 probes.

3.3 Wetting and drying tests and Monitoring

Two wetting and drying cycles were performed (additional tests are ongoing). Each cycle lasted about 10 days. At the beginning of the first wetting cycle, 10 cm of distilled water (≈ 10 liters) were added at the top of the columns to simulate precipitation. This volume represents approximately two months of precipitation in Abitibi-Témiscamingue (MELCC – Quebec climate normals 1981–2010)

The columns were left open to the atmosphere. During the 2nd wetting cycle, 5 cm of distilled water (≈5 liters) were added and fans were installed at the top of columns to increase evaporation rate.

The laboratory relative humidity and temperature were also monitored every 30 minutes using a digital hygrometer/thermometer. The temperature in the laboratory varied between 18°C and 23°C with an average temperature around 20.9°C. The relative humidity ranged from 10% to 37% (average relative humidity = 21.3%).

3.4 Numerical simulations

The study was supplemented by numerical simulations using Seep/W numerical software (GeoSlope 2019). A simplified 1D numerical model was used to simulate the hydrogeological behaviour observed within the columns. The mesh was made up of rectangular elements of 4 cm in length.

Hourly temperatures and relative humidity measured in the laboratory were applied as boundary conditions on top of the models.

The evapotranspiration model was defined using the potential evaporation rate measured in the laboratory. The volume of water used at the beginning of each cycle was converted to an equivalent water unit flux of 0.1 m/s and 0.05 m/s for the first cycle (10L) and the second cycle (5L), respectively, applied during one hour. A minimum interstitial pressure limit of –400 cm (i.e., 2*AEV of tailings) was applied to prevent excessive drying at the top of the columns.

Free drainage was allowed at the base of the models.

4 RESULTS

Static tests of the tailings revealed that the tailings were acid generating in accordance with the Guide to characterization of tailings and ore (MELCC 2020). The tailings contained more than 0.3% total sulphur (S_{total} = 9%) and a net neutralization potential (NNP) less than 20 KgCaCO3 eq/t (NNP = -259.3 $KgCaCO_3$ eq/t).

4.1 Water content evolution

The two wetting/drying cycles showed similar patterns in terms of water content variations in the tailings (Figure 5). At the beginning of a wetting cycle, the water content increases rapidly to a value close to the porosity (equivalent to Sr = 100%) and then decreases progressively with time.

During 1st cycle, probes located at 7.5 cm from the tailings surface (Figure 5 a; 5b) exhibited similar behaviour: a saturation peak was reached 3 to 6 hours after the wetting phase and was followed by desaturation as soon as this peak was reached. The saturation in column C60 was, however, slower compared to the other 3 columns (approximately 18 hours after the wetting phase). The arrival time of the wetting front (layer saturation) at the base of the columns increased with the thickness of the column (Height tailings) (Figure 5b; 5d).

The arrival times of the wetting fronts were 3h, 9h, 15h and 27h respectively for C15; C30; C45 and C60 during the first cycle. This time was reduced during the 2nd cycle for columns C60 (≈18h, i.e. -9 h) and C45 (12h, i.e. -3h), but slightly increased for columns C15 (4.5h, i.e. + 1h30) and C30 (≈ 11h, i.e. + 2h).

The second cycle started with a degree of saturation 10% higher than the first cycle for the columns C45 and C60 (it was similar in the two other columns as the first cycle). During the 2nd cycle, peak saturation was reached 3h after wetting phase for all the columns compared to the 1st cycle (i.e. -1h30 at -15h).

The vertical evolution of the degree of saturation of columns C45 and C60 during the two cycles confirmed that saturation was faster during the second cycle (Figure 6). The behaviour at the bottom of the columns was different from one column to another.

Desaturation was faster for the surface layer of the C60 column during the 2nd cycle. For column C45, desaturation began with a slight advance and was done with a small landing. After 4 days, the top layer (≈ 15 cm) was slightly less saturated in the C60 column. The C45 column reached a saturation level of 72% in the first cycle and 83% in the second cycle. Column C30 showed a similar evolution to column C45 for the surface layer.

Cracks and saline precipitates were observed at the surface of the tailings after a few days. These will be monitored and measured over the coming cycles.

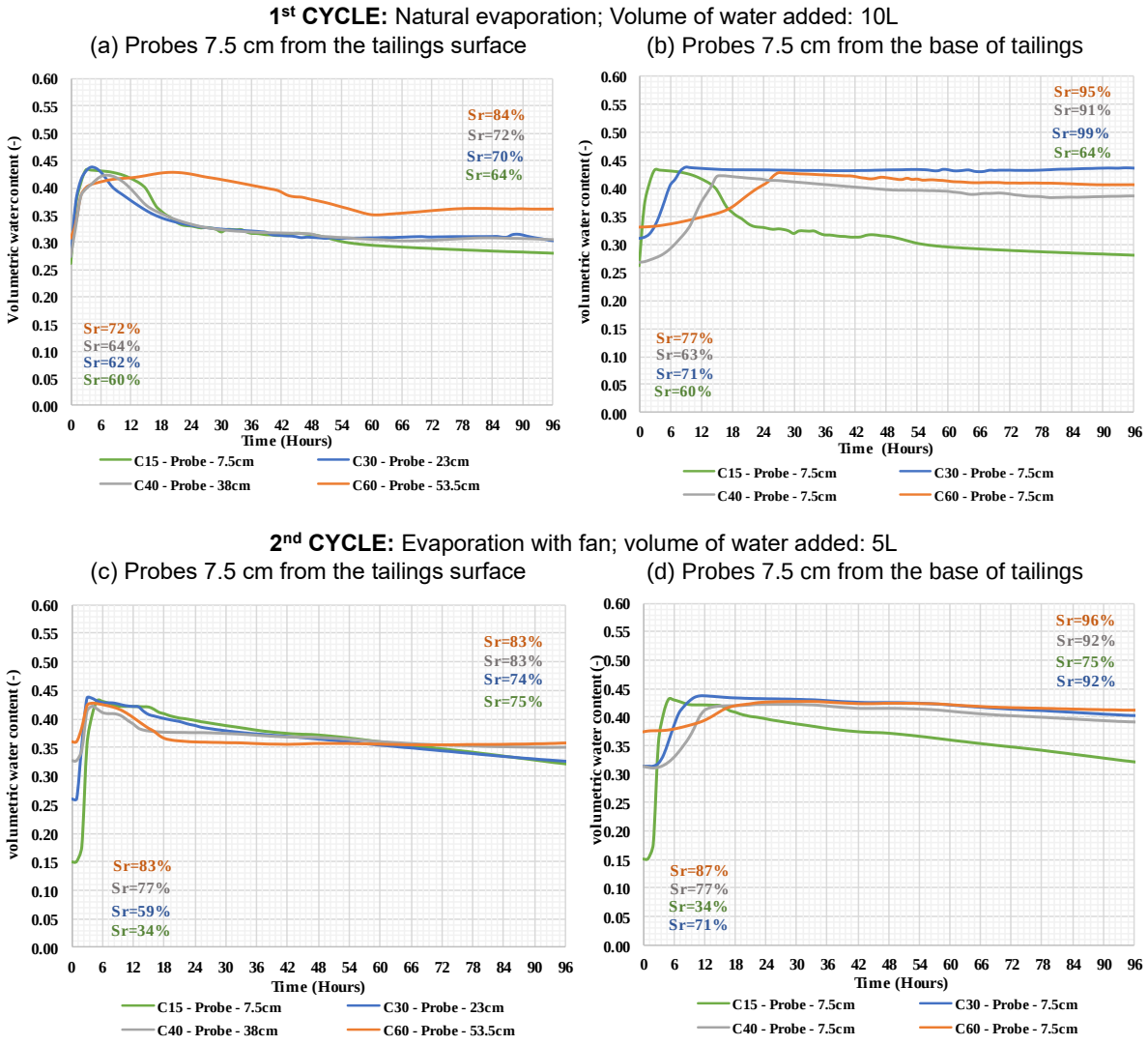

Figure 5. Evolution of the water content at the top and bottom of the four tested columns during the 1st and 2nd cycles.

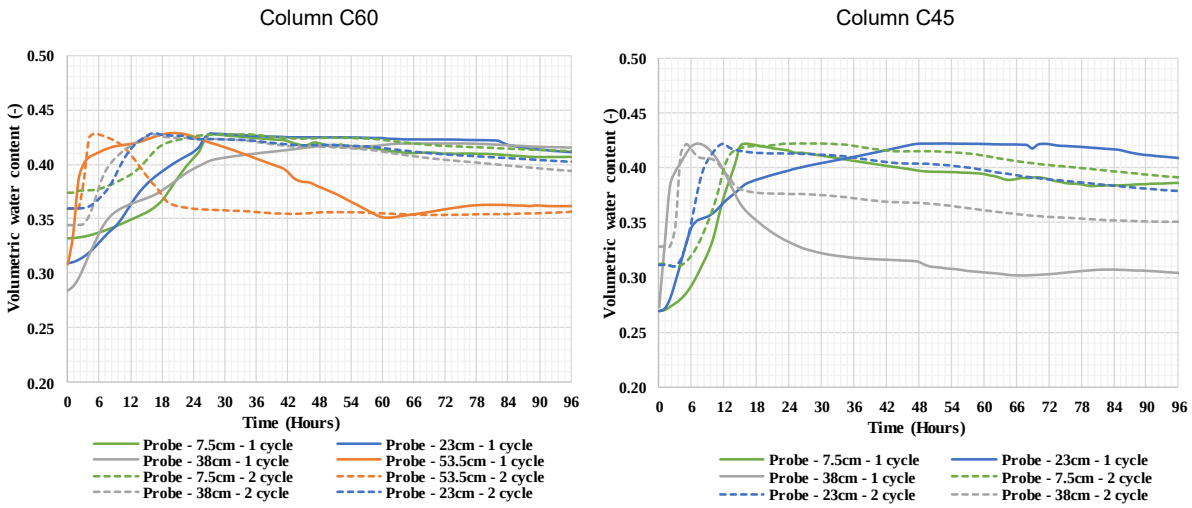

Figure 6. vertical evolution of the degree of saturation of columns C45 and C60 during cycle 1 (solid line) and cycle 2 (dashed line).

4.2 Evaporation rates with and without fans

The evaporation rate was measured during the different cycles (Table 3). Evaporation rate was similar in the 4 columns (between 1.4 and 3.5 mm/d according to the cycle). The evaporation rates measured before the wetting phase were doubled after the wetting the same cycle. This difference in evaporation rate was due to the low amount of water prior to the wetting phase. The installation of the fans at the end of the first cycle did not significantly increased the evaporation rate before the wetting phase of the second cycle.

Table 3. Measured evaporation rate in the columns with and without the fan. Potential evaporation was measured with evaporation PAN.

	1st cycle		2nd cycle	
	Evaporation rate without fan (mm/d)		Evaporation rate with fan (mm/d)	
Identification	Before wetting	After wetting	Before wetting	After wetting
C15	1.4	2.9	2.6	-*
C30	1.5	3.6	3.5	
C45	1.9	3.7	3.5	
C60	1.8	2.8	3.5	
Potential evaporation	4		7.2	

*: Not measured

4.3 Numerical simulations

The evolution of the volumetric water content in the columns was simulated using Seep/W. The results from column C60 are presented in this paper as this column had more variations (compared to the other columns) during the first wetting cycle.

The simulated volumetric water contents of the surface layer were very different from column test results. The simulated results showed a linear decrease different from the one obtained in the laboratory (desaturation is marked by a slope equivalent to Sr= -20% during the first 36 hours) (Figure 7).

The simulated results were, however, similar to the laboratory measurements for the probes placed deeper, at 38 cm; 23 cm and 7.5 cm from the base of tailings (however they showed a lower degree of saturation after 8 days). The behavior between the wetting phase and the peak saturation was not reproduced with the simulations for the whole column.

The effect of the potential evaporation rate on the top layer of column C60 was also evaluated (Figure 8). Simulations results showed that the higher the potential evaporation rate, the closer the simulated results were to those measured in the laboratory. Although a potential evaporation rate of 14mm/d showed the most similar results, this value is three times higher than that measured during the first cycle and therefore deemed little realistic. Additional simulations and laboratory tests are currently ongoing to improve the simulations.

5 RESULTS ANALYSIS AND DISCUSSION

The degree of saturation at the end of the second cycle was slightly higher than that at the end of the first cycle and close to saturation for all columns. The evaporation rates during the first cycle (without a fan) and during the evaporation cycle before the second cycle were essentially the same. The development of cracks and the formation of a layer of salts on the surface of the columns could explain the differences between measured evaporation rates before and during the first cycle. The formation of cracks at the beginning of the first cycle could have contributed to increase evaporation.

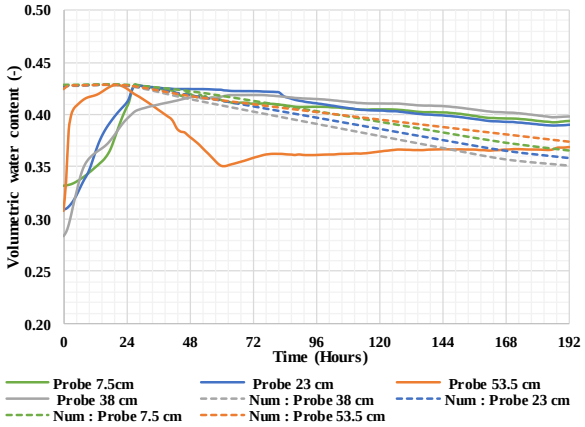

Figure 7. Measured (solid line) and simulated (dashed line) water content close to the surface of column C60 during the 1st cycle

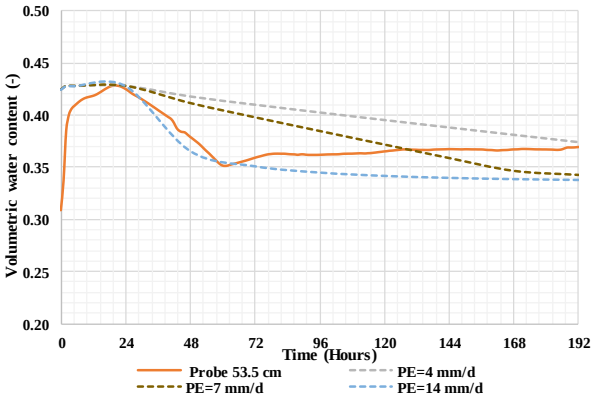

Figure 8. Influence of potential evaporation (PE) rate on the simulated water content close to the surface of column C60. Numerical results (dashed lines) are compared with measured water content (solid line).

Other research have shown that cracks can increase by two the evaporation rates (Hatano et al., 1988; Rozina et al., 2015). However, although evaporation temporarily increased with cracking it was limited by the accumulation of salts at the surface after the first cycle. Salts often create an impermeable layer which limits evaporation (Fujiyasu et al., 2000). Results also showed that the evaporation influence zone was limited to the first 25 cm below the surface. The behaviour of the deeper probes was almost identical during both cycles and for all columns. The suctions of each of the columns were followed and their evolution was compared during the different cycles (results not presented here).

Numerical simulations showed that the evaporation rate was the most critical parameter to reproduce the hydrogeological behaviour of filtered tailings. The differences between the simulated and measured results indicate that further calibration would be necessary to better represent laboratory observations and to be able to extrapolate these results to field scale.

6 CONCLUSION

Laboratory column tests were carried out to assess the hydrogeological behaviour of the filtered tailings following a series of wetting and drying cycles. The preliminary experimental results indicated that there were no significant influence of tailings thickness of the deposition layers. However, these results were based on two cycles only, and columns are ongoing to confirm these observations.

Future work will include the evaluation of compaction effects of the layers during deposition on the hydrogeological behavior. Kinetic tests and numerical simulations will also be carried out to assess the behavior of filtered tailings in the storage facilities.

ACKNOWLEDGEMENTS

The authors acknowledge the financial support from NSERC and from the partners of the Research Institute on Mines and the Environment (RIME UQAT - Polytechnique; http://rime-irme.ca/en).

REFERENCES

Aachib, M., Mbonimpa, M., & Aubertin, M. (2004). Measurement and prediction of the oxygen diffusion coefficient in partly saturated media, with applications to soil covers. *Water, Air and Soil Pollution*, *156*, 163-193.

ASTM. (2014). *Standard Test Methods for Specific Gravity of Soil Solids by Water Pycnometer*. ASTM standard D854-14.

ASTM. (2016). *Standard Test Methods for Determination of the Soil Water Characteristic Curve for Desorption Using Hanging Column, Pressure Extractor, Chilled Mirror Hygrometer, or Centrifuge*. ASTM standard D6836-16.

ASTM. (2016). *Standard Test Methods for Measurement of Hydraulic Conductivity of Saturated Porous Materials Using a Flexible Wall Permeameter*. ASTM standard D5084-16.

ASTM. (2017). *Standard Test Method for Particle-Size Distribution (Gradation) of Fine-Grained Soils Using the Sedimentation (Hydrometer) Analysis (D7928),* ASTM International, West Conshohocken, PA.

Aubertin, M., Bussière, B. & Bernier, L. (2002a). Environnement et gestion des résidus miniers. Presses Internationales de Polytechnique, Corporation de l'École Polytechnique de Montréal, Montréal. Manuel sur cédérom.

Aubertin, M., Bussière, B., Aachib, M., Chapuis, R., & Crespo, J. (1996). Une modélisation numérique des écoulements non saturés dans des couvertures multicouches en sols. *Hydrogéologie, 1*, 3-13.

Azam, S. & Li, Q., (2010). Tailings Dam Failures: A Review of the Last One Hundred Years. *Geotechnical News*, December 2010.

Bouzahzah, H. 2013. Modification et amélioration des tests statiques et cinétiques pour une prédiction fiable et sécuritaire du drainage minier acide. Thèse de doctorat, Université du Québec en Abitibi-Témiscamingue (UQAT), 274 p.

Bussiere, B. (2007). Colloquium 2004: Hydrogeotechnical properties of hard rock tailings from metal mines and emerging geoenvironmental disposal approaches. *Canadian Geotechnical Journal*, *44*(9), 1019-1052. doi:10.1139/T07-040

Fourie, A (2012b). Perceived and realised benefits of paste and thickened tailings for surface deposition. In R.J. Jewell, A.B. Fourie, & A. Paterson (eds.), *Paste 2012: Proceedings of the 15th International Seminar on Paste and Thickened Tailings* (p.53-64). Perth, Australia: Australian Center for Geomechanics.

Fredlund, M. D., Fredlund, D., & Wilson, G. W. (2000). An equation to represent grain-size distribution. *Canadian Geotechnical Journal, 37*(4), 817-827.

Fujiyasu, Y. & Fahey, M. (2000) *Experimental* study of evaporation from saline tailings. *Journal of Geotechnical and Geoenvironmental Engineerin*g, 126: 18–27.

Hatano, R., Nakamoto, H., Sakuma, T. & Okajima, H. (1988): Evapotranspiration in cracked clay field soil. Soil Sci. Plant Nutrition, 34(4), 547–555.

James, M., Aubertin, M., & Bussière, B. (2013). On the use of waste rock inclusions to improve the performance of tailings impoundments. *Proc. 18th International Conference on Soil*

Mechanics and Geotechnical Engineering, Paris, France, pp. 735-738.

Lindsay, M. B., Moncur, MC., Bain, J. G., Jambor, J. L., Ptacek, CJ., & Blowes, DW. (2015). Géochimique et aspects minéralogiques de sulfure mien les résidus. Appliqué Géochimie, 57, 157-177.

Maqsoud, A., Mbonimpa, M., & Bussière, B. (2013). Réhabilitation du site minier abandonné Aldermac : résultats préliminaires du suivi de la nappe surélevée. Communication présentée *à GeoMontréal*, Montréal.

Martin, V. (2018). Evolution of the Hydrogeotechnical Properties of Paste Tailings Deposited on the Surface. Thèse de doctorat, École Polytechnique de Montréal.

Mend (2009). Report 1.20.1 Prediction manual for drainage chemistry from sulphidic geologic materials.

Ministère de l'environnement et de la lutte contre les changements climatiques (MELCC 2020) : Guide to characterization of tailings and ore, Quebec, 52 p. [Online].

Morin, K. A., & Hutt, N. M. (2001). Environmental geochemistry of Minesite drainage: *Practical theory and case studies*. Vancouver: MDAG Pub.

Nordstrom, DK., Blowes, DW., & Ptacek, CJ. (2015) Hydrogeochemistry and microbiology of mine drainage: An update. Applied Geochemistry 57: 3-16

Pabst, T., Aubertin, M., Bussière, B. & Molson, J. (2017). Experimental and numerical evaluation of single-layer covers placed on acid-generating tailings. *Geotechnical and Geological Engineering, 35*(4), 1421-1438

Pabst, T., Bussiere, B., Aubertin, M. & Molson, J. (2018). Comparative performance of cover systems to prevent acid mine drainage from pre-oxidized tailings: A numerical hydro-geochemical assessment. *Journal of Contaminant Hydrology, 214*, 39-53.

Robinsky, E.I. (1975). Thickened discharge – A new approach to tailings disposal. CIM Bulletin. 68 :764. 47-56.

Robinsky, E.I. (1999). *Thickened tailings disposal in the mining industry*. Toronto, Ontario: E.I. Robinsky Associates Ltd. 210p.

Rozina, E., Mizani, S., Malek, M., Sanchez, M., & Simms, P. (2015). *Desiccation and consolidation in a laboratory simulation of multilayer deposition of oil sands fine tailings*. In Proceedings of Paste 2015, Cairns, Australia, 5–7 May 2015.

Spitz, K., & Trudinger, J., 2009. *Mining and the Environment:* From Ore to Metal. CRC Press 891p.

Strachan, C. & Goodwin, S. (2015) The Role of Water Management in Tailings Dam Incidents. Proceedings, *Tailings and Mine Waste 2015*; Vancouver, British Columbia, October 26-28.